EFFECT OF FINITE ELEMENT CHOICE IN BLUNT CRACK BAND ANALYSIS

Luigi CEDOLIN

Associate Professor, Politecnico di Milano, Italy; formerly Visiting Scholar, Northwestern University

Zdeněk P. BAŽANT

Professor of Civil Engineering, Northwestern University, Evanston, Illinois 60201, USA

The previously developed method of element-wide blunt smeared crack bands, which allows an effective finite element analysis of cracks that are not fixed but propagate and do so in any direction, has so far been numerically studied and demonstrated only for the constant-strain triangular elements. Here this is accomplished for linear strain triangles and for all three methods developed in [1], including the methods of energy variation, of equivalent strength, and of fitting asymptotic series to nodal displacements. Meshes of greatly different sizes are shown to give again the same results except for a negligible error; this indicates satisfactory convergence. Accuracy of the stress intensity factor, compared to the exact solutions for sharp cracks, is found to be sufficient but not better than that achieved previously with constant strain triangles. However, the accuracy may well be better in case of concrete structures in which the element-wide crack band serves not merely as a convenient approximate representation of a sharp crack but as a better representation of the actual fracture process.

Introduction

Sharp interelement cracks represent a very cumbersome and prohibitively difficult approach to model the crack propagation, especially when the crack path is not known in advance. When the crack extends through a certain node, this node doubles as two nodes, the topology (or connectivity) of the finite element mesh changes and the nodes must be renumbered. The renumbering may be avoided by treating the nodes that are to fracture later as two coincident nodes constrained together until the crack extends through the node; but this is useless when we do not know beforehand through which nodes the crack is going to pass. When the crack direction is unknown, the node location cannot be considered fixed and the calculations must be run for various node locations.

Concrete engineers have long used a much more effective approach. In keeping with the physical reality in concrete structures, they model fracture as bands of parallel cracks continuously distributed or smeared through the whole finite element. All that one has to do to represent cracking is to change the element stiffness matrix assuming that the material

becomes orthotropic, with the modulus for extension normal to the cracks being reduced to zero. In this manner one can easily extend the crack band into any element and one can easily model cracks of any direction, without considering nodes of different locations.

This traditional approach suffers, however, from a fundamental fault: it is not objective because the results depend on our choice of finite element size and do not converge as the element is shrunk to zero in size. This is because one extends the crack into the next element on the basis of a strength criterion. If we note that the crack front has always the width of a single element (which can be shown by analyzing unstable localization of strain due to cracks) we see that the crack front becomes sharper and sharper as the mesh is refined, causing stress concentration. Thus, the stress in the element just ahead of the crack front tends to infinity no matter how small is the applied load. So we conclude that using the strength criterion we can obtain extension of the existing crack band for as small a load as we please. The only reason that many practical calculations of reinforced concrete beams, slabs and panels have been satisfactory is that the element size has been about the smallest admissible one in relation to material inhomogeneities, i.e., the aggregate size. This is not so, however, when large structures, for example dams or reactor vessels, are to be analyzed.

The only way to eliminate such spurious dependence of fracture predictions on the chosen element size is to adopt the fracture mechanics approach in which the crack propagation is based on the fact that the work consumed as the crack or the crack band is extended by a unit length is a constant. The concept of element-wide blunt smeared crack bands was founded on this fracture mechanics criterion in a previous paper [1], in which a survey of pertinent literature can also be found. One direct and two indirect methods of implementing the energy criterion of crack propagation, each with its own special computational advantages and disadvantages, were proposed and numerically demonstrated. It was shown that fracture predictions of sufficient practical accuracy can be obtained for relatively crude regular meshes without mesh refinement near the crack front.

One rather interesting result was that for constant strain triangular elements the element-wide blunt crack band yields the stress intensity factor with about the same accuracy as the sharp interelement crack used so far in fracture mechanics. It is certainly rather useful to know that there is very little difference between a sharp crack and an element-wide crack band. We must keep in mind, though, that the modeling of sharp cracks with the element-wide crack bands is not the only objective. In certain structures, such as concrete structures or rock masses, we do actually have bands of cracks rather than sharp isolated cracks.

All results in the previous paper [1] were obtained with the simplest elements, the constant strain triangular elements. We will therefore examine here what is the effect of choosing higher-order finite elements, such as linear strain triangles, and whether the accuracy equivalence of element-wide blunt crack bands and sharp interelement cracks still holds for the higher-order elements. We will study this question for all three methods developed in [1].

The finite element calculations in [1] were performed with four-node quadrilateral elements composed of two constant strain triangles (CST). This type of element is widely used in practical nonlinear analysis of reinforced concrete structures and the calculation of its stiffness is very simple.

In this work, we choose the six-node linear strain triangles (LST). To be able to use the same meshes as before [1], we arrange four triangles to form a quadrilateral element, same as used before [1]. In this quadrilateral element, the efficacy of which is well known [2], the five

nodes inside the quadrilateral are eliminated by static condensation. For convenience, the exterior midside nodes are also eliminated by constraining the displacement variation along the sides of quadrilateral to a linear one, so that the element may be treated as a four-node quadrilateral.

1. Method A. Energy variation due to crack band advance

As shown in [1], the energy release that takes place as a crack band advances by one element may be calculated as

$$\Delta U = \frac{1}{2} \int_{\Delta S} \Delta T_i (u_i - u_i^0) \, dS + \Delta W_{(\Delta V)}, \tag{1}$$

with

$$\Delta W_{(\Delta V)} = -\frac{1}{2} \int_{\Delta V} (\sigma_{ij}^0 \epsilon_{ij}^0 - E' \epsilon_{11}^{02}) \, dV, \tag{2}$$

in which the subscripts i, j $(=1, 2)$ refer to cartesian coordinates x_1 and x_2 with x_1 aligned with the crack band (fig. 1), ΔV is the volume (or area) of the finite element into which the crack band advanced, ΔS is the surface (or length) of the boundary of this element, ΔT_i are the nodal forces which must be externally applied on ΔS to the remaining part of the body in order to preserve the initial stress state while the crack propagates into ΔV, u_i and u_i^0 are the nodal displacements after and before the crack band advances, respectively, σ_{ij}^0 and ϵ_{ij}^0 are the stresses and (small) strains that exist in volume ΔV before the crack band advances, $\Delta W_{(\Delta V)}$ is the energy loss due to release of stresses in ΔV, and the remaining term in eq. (1) is the energy loss of the surrounding grid released into ΔV.

For the case of plane stress we have $E' = E$, where E = Young's modulus, while for the case of plane strain we have $E' = E/(1 - \nu^2)$, where ν is Poisson's ratio. The energy release rate $\mathcal{G}$ may be approximated as $-\Delta U/\Delta a$, and the (mode I) stress intensity factor may be calculated as

$$K_I = \sqrt{E'\left(\frac{-\Delta U}{\Delta a}\right)}, \tag{3}$$

where Δa is the length of crack band advance (fig. 1d).

The results for the element-wide blunt crack band obtained with the meshes shown in fig. 1e are exhibited in fig. 2. Case (a) pertains to a straight crack of length $2a$ within an infinite solid subjected at infinity to a homogeneous uniaxial tensile stress $\bar{\sigma}$ normal to the crack (fig. 1a). Only a domain of finite size within the infinite solid is solved by finite elements (fig. 1e) and the forces applied at the boundary nodes of this domain are the resultants of the exact stresses acting at this boundary, calculated according to Westergaard's exact solution [1]. Case (b) pertains to a straight crack of length $2a$ symmetrically located within a finite strip of length $2L$ and width $2b$, subjected at the ends to homogeneous uniaxial tension $\bar{\sigma}$ along the strip (fig. 1b). The computations are carried out for $E' = 225\,600\,\text{MN/m}^2$, $\nu' = 0.2$ and the critical value
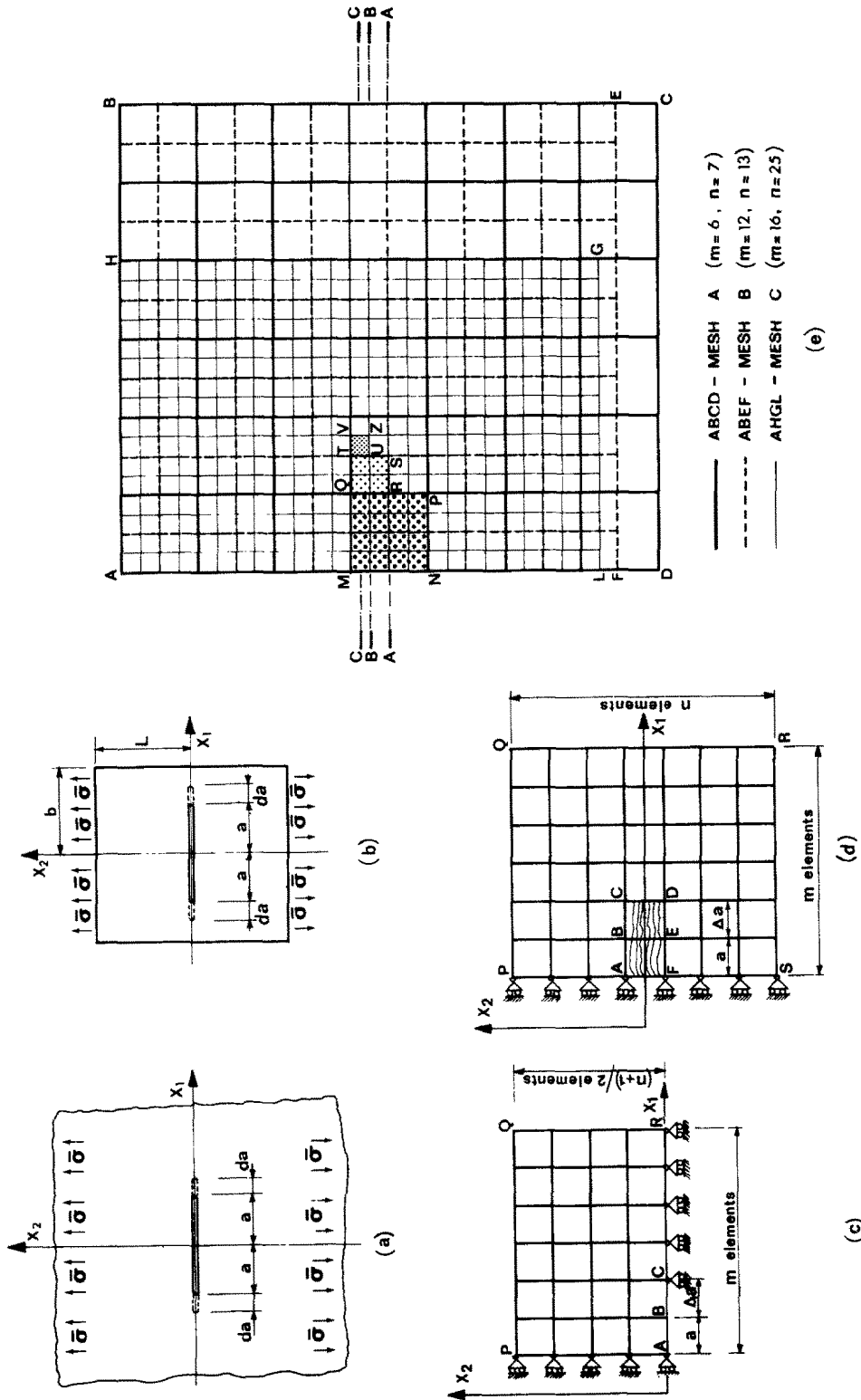
Fig. 1. (a) Crack in infinite solid: (b) Crack in finite strip; (c) Finite element mesh used for sharp interelement crack; (d) Finite element mesh used for blunt-crack band; (e) Mesh refinements used in examples.
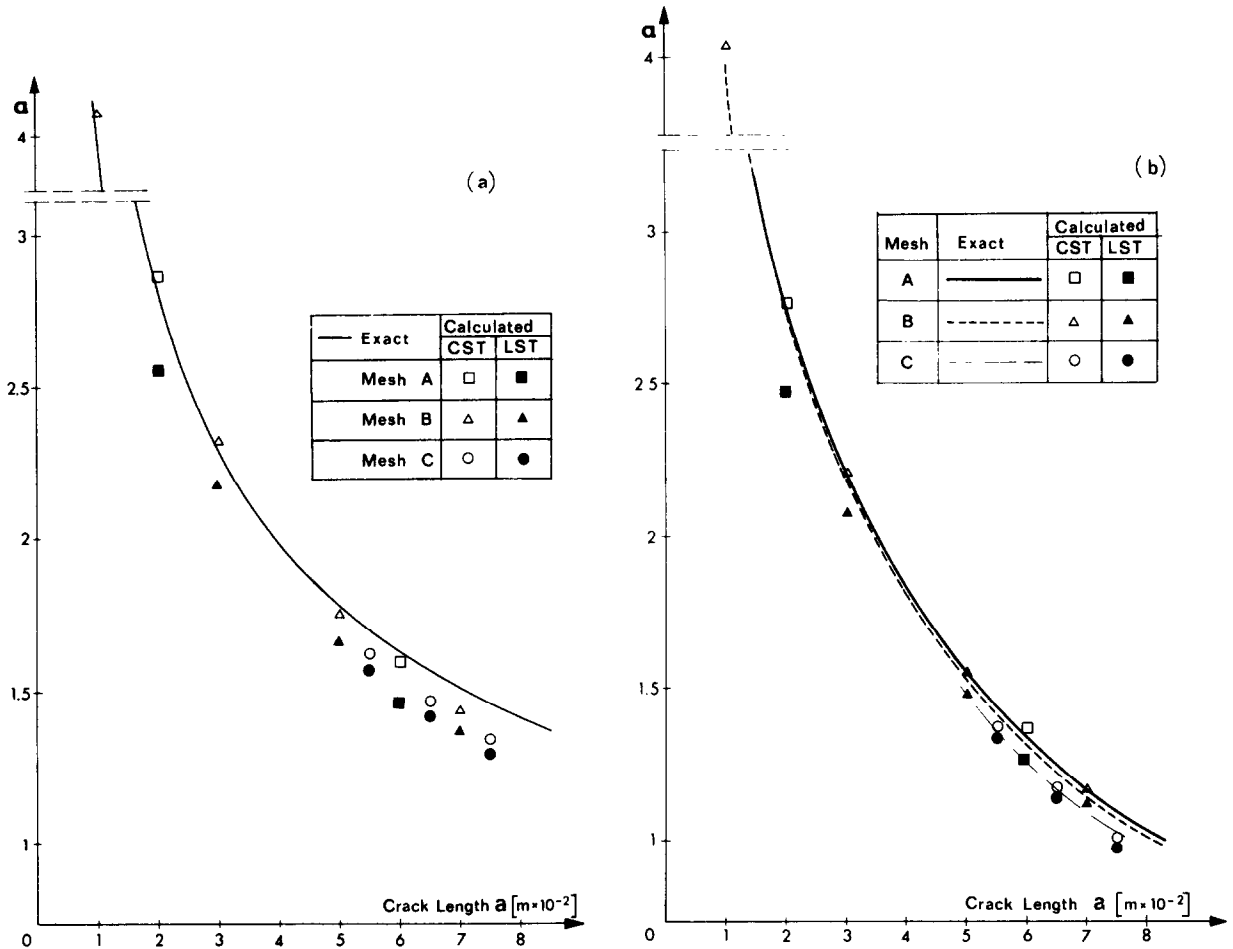
Fig. 2. Comparison of numerical results from energy variation with exact solution for blunt-crack band: (a) Infinite solid; (b) Finite strip (α = load multiplier) (1 m = 3.28 ft).

$K_{cr} = 0.6937$ MN m$^{-3/2}$ of the stress intensity factor K_1. The applied uniaxial stress is assumed as $\bar{\sigma} = 0.981$ MN/m^2. The ordinates in fig. 2 as well as in several subsequent figures are the critical values of the applied stress multiplier α such that $\alpha\bar{\sigma}$ is the stress that causes crack propagation.

Similar results for a sharp interelement crack (fig. 1c) are given in figs. 3a, 3b.

In figs. 2 and 3 we first of all note that the results for various mesh sizes tend to fall near the same curve. This indicates to us satisfactory convergence. By contrast, this is not the case when the crack band is propagated on the basis of the strength criterion, as has been demonstrated in [1] where a 90% difference was found between the α-values for meshes A and C.

From the comparison in figs. 2 and 3 between the results for the constant strain triangles (CST) and for the linear strain triangles (LST) we see that the latter ones always give smaller α-values, i.e. smaller values of the load that is necessary for propagation. This is true both for the element-wide blunt crack band and the sharp interelement crack. The reason obviously
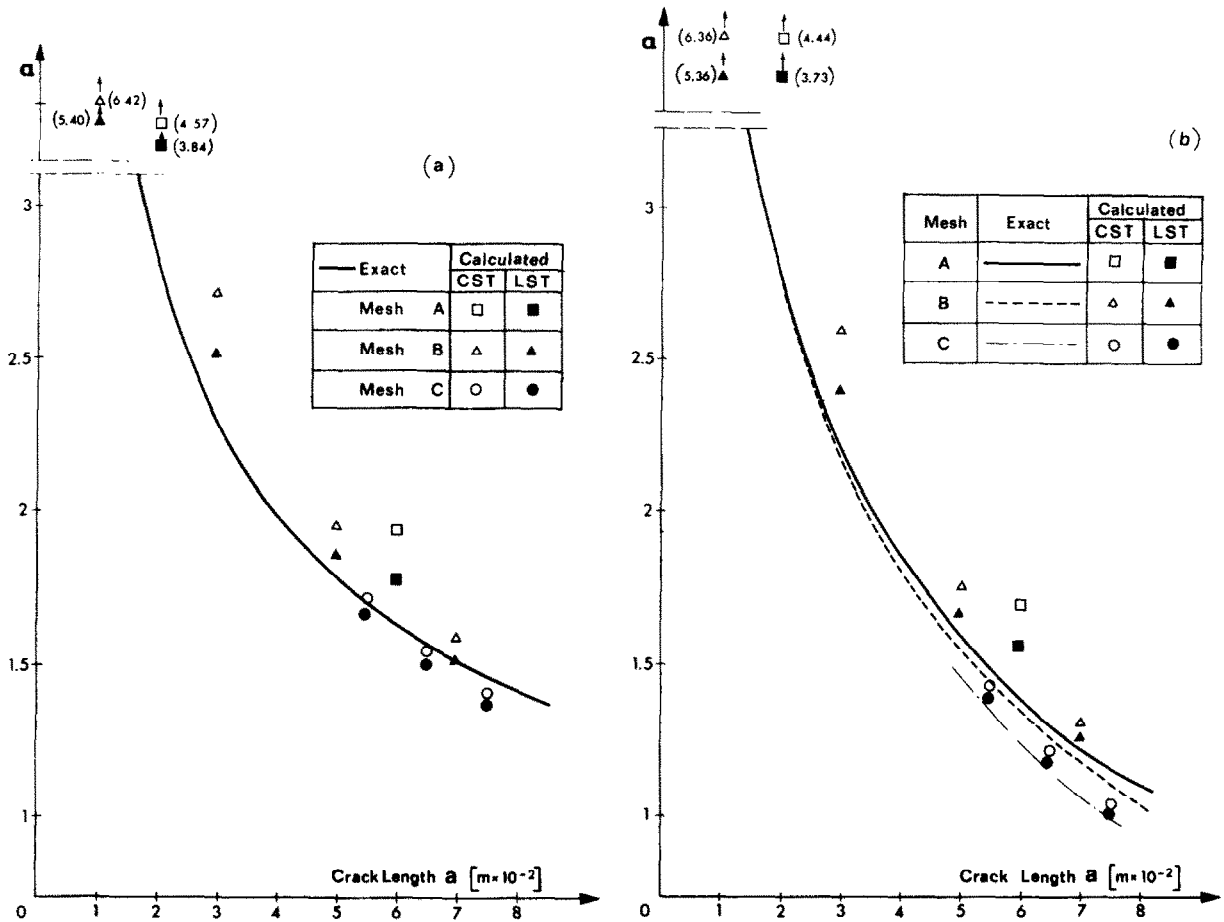
Fig. 3. Comparison of numerical results from energy variation with exact solution for sharp interelement crack: (a) Infinite solid; (b) Finite strip (1 m = 3.28 ft).

consists in the fact that, as is well known, the CSTs are generally stiffer than the LSTs, which causes that the calculated crack openings, as well as both work terms in eq. (1), are smaller for CSTs. Because the CST results for the blunt crack band have generally a negative error which puts them on the low side, a switch from CST to LST tends to impair accuracy, compared to the exact solution (figs. 2a, 2b). On the other hand, for sharp interelement cracks we see an improvement of accuracy because the CST results have generally a positive error which puts them on the high side.

We may now observe that the element-wide blunt crack band generally gives somewhat smaller α-values (i.e. softer response) than the sharp interelement crack, as compared to the exact solution for a sharp crack. This error type tends to compensate for the error caused by the high stiffness of CST, and this is why the CST results for element-wide blunt crack band, appear to be so good, and in fact slightly better than the LST results, as compared to the exact solution for a sharp crack. In case of the LSTs, these two types of error do not quite cancel each other because the positive error due to the element type is smaller, and this is why the LST results for the element-wide crack bands appear to be slightly worse than those for the sharp interelement cracks.

This is of course true only when we compare with the exact solution for a sharp crack. For inhomogeneous structures, such as reinforced concrete structures, propagation of crack bands actually precedes the formation of isolated final cracks. Comparison with the exact solution for a sharp crack is then not quite relevant. Rather, the results should be compared to the correct solution for a blunt crack band of the correct band width, but such solutions are not yet known. Nevertheless the blunt crack band solution with LST is likely to be more correct than that with CST.

2. Method B. Equivalent strength criterion

In this method we approximate the energy variation due to the crack front advance in terms of the stress in the element that undergoes cracking. Since the stress within the quadrilateral element is not constant and the whole element consisting of four triangles cracks simultaneously, we must base the energy loss calculation on some average value of stress within the quadrilateral element. The average stress σ_{22}^0 at the central point C of the quadrilateral element V (PQRS in fig. 4c) may be adopted for this purpose.

According to eqs. (15) and (16) of [1] the energy loss may be approximated as

$$\Delta W_{(\Delta V)} \approx - \frac{hw}{2E'} (\sigma_{22}^0)^2, \tag{4}$$

where h is the element length (length of advance of the crack band), and w is the element width (width of the crack band). The work of nodal forces acting on the element PQRS (fig. 4c) from the surrounding grid may be approximated, according to eq. (17) of [1], as

$$\frac{1}{2} \int_{\Delta S} \Delta T_i (u_i - u_i^0) \, \mathrm{d}S \approx - \frac{h}{4} \sigma_{22}^0 (u_P - u_Q), \tag{5}$$

where u_P and u_Q are the vertical displacements of nodes P and Q in fig. 4c. Recalling the asymptotic expansion of displacements near the tip of a sharp crack, we may further set

$$u_P - u_Q \approx \frac{8}{E'} \frac{K_I}{\sqrt{2\pi}} \sqrt{w}. \tag{6}$$

If we substitute this into eq. (5), then substitute eqs. (5) and (4) and set $\Delta U = -K_I^2(h/E')$, we obtain the equation

$$- \frac{h}{E'} K_I^2 = - \frac{h}{4} \sigma_{22}^0 \frac{8}{E'} K_I \sqrt{\frac{w}{2\pi}} - \frac{hw}{2E'} (\sigma_{22}^0)^2, \tag{7}$$

which is a quadratic equation in σ_{22}^0. This equation has only one positive solution, which yields the approximation

$$(\sigma_{22}^0)_{cr} = \sigma_{eq} = K_{cr} \frac{c}{\sqrt{w}}, \qquad \text{with } c = 0.826, \tag{8}$$

where K_{cr} is the critical value of K_I at which the crack propagates. Eq. (8) is the same as eq. (21) in [1] applicable for CST except for a different value of constant c. In fact, the form of eq. (8) is general, and the constant c is characteristic of the particular type of elements at the crack front.

Eq. (8) shows that there exists a critical value σ_{eq} of the stress at the element centroid for which the crack propagates. This value is called the equivalent strength [1]. In the usual practice of finite element analysis of crack propagation in concrete structures [1] a constant strength value has been used in the propagation criterion, but from eq. (8) we see that the strength value cannot be considered as constant but must be decreased if the width of the finite element at crack front is diminished.

If this is not done, convergence does not take place as the grid is refined, and as the element width tends to zero the load needed to propagate the crack tends to zero, rather than a finite value. This property is obviously incorrect. In fig. 5a of [1] one finds an example where the error in the load needed for propagation is about 100% if the element width is decreased four times. A similar example of an error incurred when the same strength is considered for different meshes is plotted for LST in fig. 4a. Since the ratio of the sizes of meshes A and C is $4:1$, σ_{eq} for mesh A should be $\sqrt{4}$ times higher, and so the error is 100% if the same σ_{eq} is considered.

The values of the load multiplier α, which is obtained with the equivalent strength criterion (8), are plotted in figs. 4a, 4b for the infinite medium and the finite strip. The comparison with the results of the energy criterion, made in the same figure, shows that somewhat higher values of α are obtained. Inspecting the numerical results, we find that this overestimation appears to originate from the fact that eq. (5) tends to underestimate the work of the surface tractions. This is because the nodal forces at P and Q are calculated on the basis of the average stress at the centroid, σ_{22}^0, while the actual stress distribution inside the element will be increasing in the direction toward the crack front (side PQ in fig. 4c).

Eqs. (4)–(6), from which the equivalent strength criterion is derived, are of course only approximate. More accurately, one may assume only the general form of eq. (8), which is a basic property, and calibrate the value of c by some trial case for which we know the exact solution.

Comparing the results in figs. 4a, 4b with those obtained with CSTs (figs 5a, 5b of [1]), we note that the deviation in sign is opposite to the one found for method A. This is due to the fact that, although the calculated displacement $u_P - u_Q$ is greater owing to the higher flexibility of LSTs, the aforementioned underestimation of the nodal forces at P and Q nodes is more significant and prevails in determining the sign of the error in the work of the surface tractions. This work, as mentioned for method A, gives the largest contribution to the energy release as the crack advances.

3. Method C. Fitting asymptotic series to nodal displacements

In this method the nodal displacements U, V obtained for a blunt smeared crack band are fitted by the asymptotic series expansion for a sharp crack tip, which gives the displacements as functions [1] of the first four series coefficients d_1, d_2, d_3, d_4, the crack tip displacements U_T, V_T, the crack tip coordinates X_T, Y_T, and the crack direction α. The coefficient of the leading
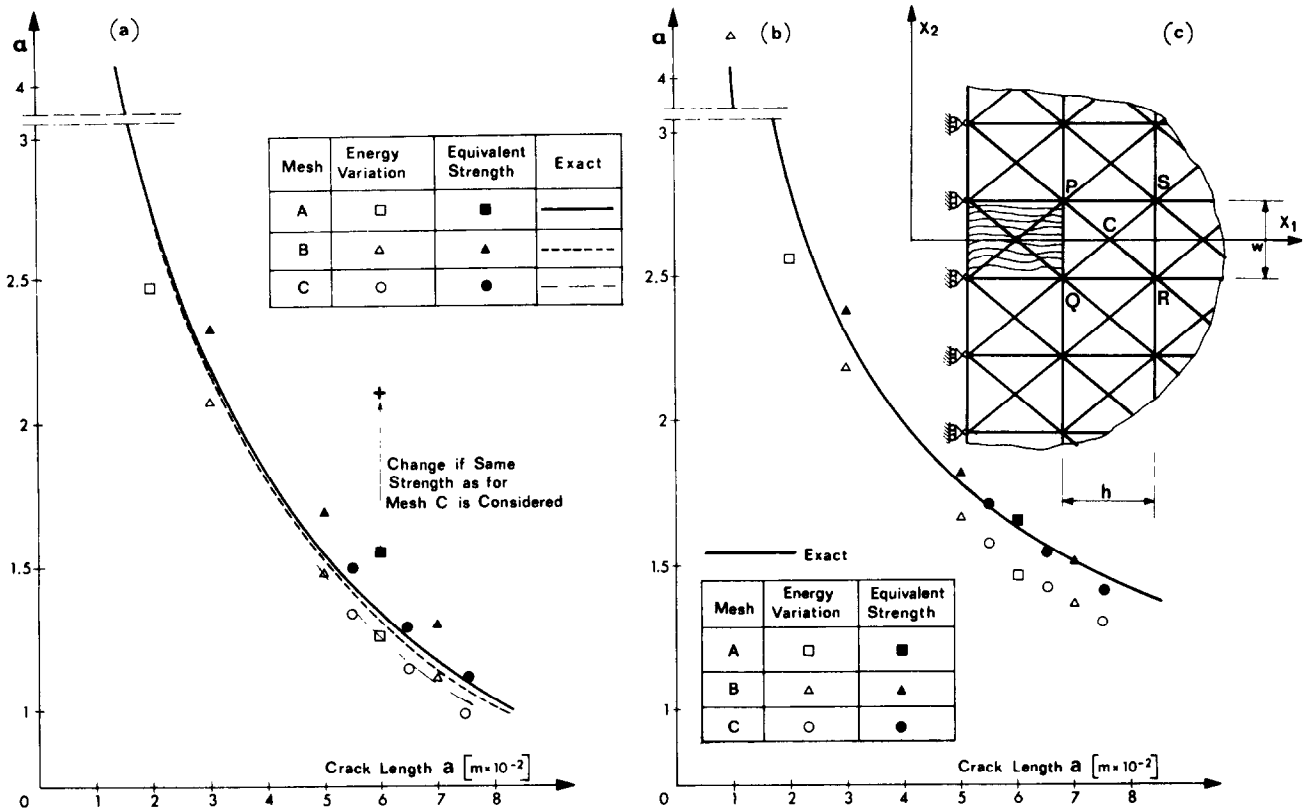
Fig. 4. Blunt crack comparison between energy variation and equivalent strength criteria: (a) Finite strip; (b) Infinite solid; (c) Mesh detail at front of blunt-crack band (1 m = 3.28 ft).

term, d_1, is linearly related to the stress intensity factor K_1 [1]. The dependence of displacements on parameters X_T, Y_T and α is nonlinear. The optimum fit of nodal displacements may be determined by using an optimization method (such as the Marquardt–Levenberg algorithm) to minimize the sum of square deviations from the nodal displacements. In the present numerical work, parameters Y_T and α (fig. 5b) have not been considered as unknowns, being set equal to zero, because the attention centered on the effect of using higher-order finite elements.

The proper choice of the characteristic nodes whose displacements are to be fitted was discussed in [1] (one possible selection is shown in fig. 5a). Here we are interested in assessing the effect of the use of LSTs on the accuracy of determining the stress intensity factor and crack tip location. The crack opening profiles calculated with the help of CSTs and LSTs are shown in fig. 5c. Since LST is more flexible than CST, a wider crack opening may be expected, and this is confirmed by the numerical results in fig. 5c. Because the crack opening in the vicinity of the crack tip is proportional to the stress intensity factor, we thus may expect a larger value of the stress intensity factor when we switch from CST to LST.

The crack tip locations X_T and the values of coefficient $c_1 = -(K_1/2G)/\sqrt{2\pi}$ characterizing K_1 are tabulated in table 1 for five different selections of characteristic points shown in fig. 6. We see that indeed the values of c_1 as well as X_T are generally on the high side and are larger
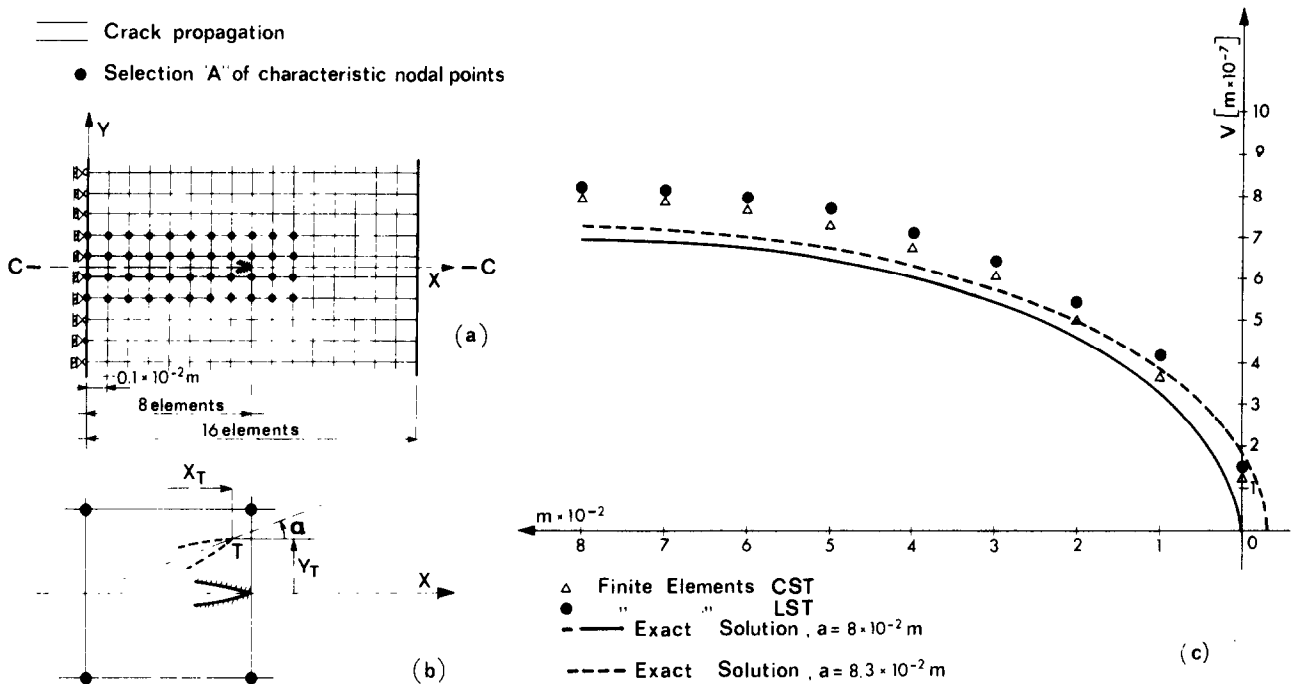
Fig. 5. (a) Example studied by asymptotic expansion fitting; (b) Change in direction of propagation; (c) Crack opening profile obtained (1 m = 3.28 ft).

than the exact values for a sharp crack. Thus, curiously, the use of LST does not improve the accuracy of calculation of the stress intensity factor. Apparently, the numerical error of CST is opposite to the error in crack representation and tends to cancel it, whereas the error of LST is too small to cancel the latter error.

4. Interpretation of results and conclusions

The previously developed method for modeling cracks as element-wide blunt smeared crack bands has so far been numerically demonstrated only for the constant strain triangular

Table 1. Typical numerical results for method C

Node selection	X_T (cm)		$C_1 \times 10^5$ (cm$^{1/2}$)	
	CST	LST	CST	LST
Exact	8.000	8.000	−1.043	−1.043
A	7.885	7.978	−1.190	−1.246
B	7.937	8.101	−1.164	−1.204
C	7.950	8.194	−1.156	−1.176
D	7.967	8.235	−1.144	−1.154
E	8.090	8.343	−1.065	−1.104

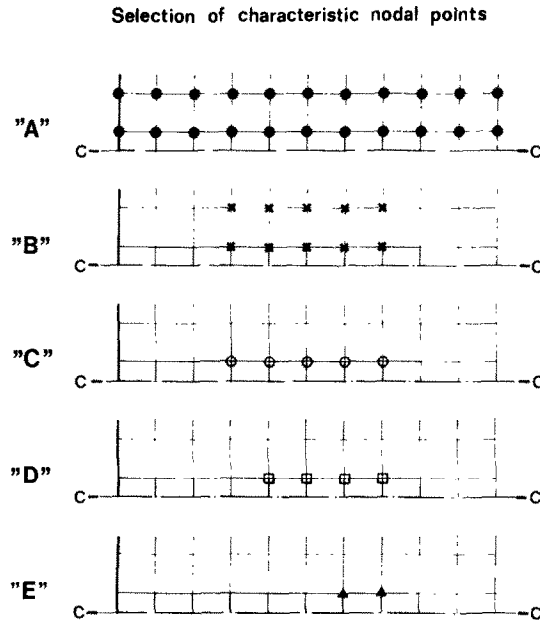Selection of characteristic nodal points

Fig. 6. Various selections of characteristic points.

elements. The present work validates the method for higher-order finite elements, particularly the linear strain triangles.

One objective has been to demonstrate convergence, i.e., show that meshes of greatly different sizes give the same results except for a negligible error. The practically found convergence for linear strain triangles is found to be indeed satisfactory for all three methods.

The second and main objective has been to assess the accuracy of crack propagation calculations with higher-order finite elements. Exact solutions for checking the accuracy are available only for sharp cracks in a homogeneous continuous medium. If that is the yardstick, it appears that the linear strain triangles do not allow a better accuracy than the constant strain triangles, the use of which is much simpler. This is true of the basic approach through the release rate of energy of the crack band extension, as well as of the alternate approaches through the equivalent strength or the asymptotic series expansion of the displacement field near the crack front. For the latter two approaches the computational results are actually worse than those obtained previously with the constant strain triangles. This is because there are two sources of error giving errors of opposite sign. The use of a crack band of a finite width makes the response softer while the use of conforming elements makes the response stiffer than the exact one. If constant strain triangles are used, the element error just about offsets the error due to the crack band, but if linear strain triangles are used, the element error becomes too small to offset the error due to the crack band. Obviously, the improvement in element accuracy does not suffice to improve the overall accuracy of fracture calculation; it would be necessary to also improve the representation of crack band propagation. Compared to a sharp crack, we introduce error by assuming a fixed finite width of the crack band, and also by assuming that the entire quadrilateral element consisting of four triangles at the crack front cracks simultaneously. Actually, the cracks must spread through this quadrilateral

element gradually, and only if such a model were available one might expect better overall accuracy of fracture calculations with higher-order elements.

If the exact solutions for a sharp crack are not the ultimate yardstick, as is the case for inhomogeneous structures such as reinforced concrete structures, the linear strain triangles are most likely superior to constant strain triangles in these fracture calculations because the stiffness of the structure is more accurately represented and the band of cracks in concrete is modeled as an actual crack band in the grid. It is in such situations where the use of higher-order finite elements is appropriate.

On the other hand, if the element-wide blunt crack band is used to model the growth of sharp isolated cracks, it is preferable to refrain from introducing the higher-order finite elements, except possibly in the regions remote from the crack tip.

From the viewpoint of various convergence concepts, our numerical solutions demonstrate convergence to the exact solution if the mesh is refined, which is called the h-convergence. It seems, however, that we do not have the so-called p-convergence as the order of interpolating polynomial (basis functions, shape functions) of the finite element is increased, and in this spirit the present method seems to lack objectivity. This may be considered disturbing. From the modeling viewpoint this may be nevertheless, expected because the crack band does not tend to coincide with a sharp crack no matter how high is the degree of the interpolating polynomial in the finite element. The p-convergence may well exist, as our numerical results suggest, but it is a convergence to a certain solution other than the sharp crack solution. In view of the fact that there actually is a crack band at the front of a crack in a heterogeneous material such as concrete, the aforementioned nature of p-convergence in our problem does not seem unreasonable. On the other hand, if we seek to model sharp cracks rather than blunt crack bands in concrete, the p-convergence is apparently not achieved without formulation and some procedure to shrink the band width as the polynominal order is increased would have to be devised.

Acknowledgment

References

[1] Z.P. Bažant and L. Cedolin, Blunt crack band propagation in finite element analysis, J. Eng. Mech. Div., Proc. ASCE 105 (1979) 297–315.
[2] C.A. Felippa, Refined F.E. analysis of linear and nonlinear two-dimensional structures, Ph.D. Diss., Univ. California, Berkeley, CA, 1966.